David Taylor Research Center
Bethesda, MD 20084-5000

DTRC-88/006 February 1988

Ship Electromagnetic Signatures Department
Research and Development Report

Thermal Macrowake of Surface Ships

by

Peter O. Cervenka

MAJOR ORGANIZATIONAL COMPONENTS

CODE 011 DIRECTOR OF TECHNOLOGY, PLANS AND ASSESSMENT

12 SHIP SYSTEMS INTEGRATION DEPARTMENT

14 SHIP ELECTROMAGNETIC SIGNATURES DEPARTMENT

15 SHIP HYDROMECHANICS DEPARTMENT

16 AVIATION DEPARTMENT

17 SHIP STRUCTURES AND PROTECTION DEPARTMENT

18 COMPUTATION, MATHEMATICS & LOGISTICS DEPARTMENT

19 SHIP ACOUSTICS DEPARTMENT

27 PROPULSION AND AUXILIARY SYSTEMS DEPARTMENT

28 SHIP MATERIALS ENGINEERING DEPARTMENT

UNCLASSIFIED

SECURITY CLASSIFICATION OF THIS PAGE

REPORT DOCUMENTATION PAGE

1a REPORT SECURITY CLASSIFICATION Unclassified	1b RESTRICTIVE MARKINGS
2a SECURITY CLASSIFICATION AUTHORITY	3 DISTRIBUTION / AVAILABILITY OF REPORT Approved for public release; distribution is unlimited.
2b DECLASSIFICATION / DOWNGRADING SCHEDULE	
4 PERFORMING ORGANIZATION REPORT NUMBER(S) DTRC-88/006	5 MONITORING ORGANIZATION REPORT NUMBER(S)
6a NAME OF PERFORMING ORGANIZATION David Taylor Research Center 6b OFFICE SYMBOL (*If applicable*) Code 1412	7a NAME OF MONITORING ORGANIZATION
6c ADDRESS (*City, State, and ZIP Code*) Bethesda, MD 20084-5000	7b ADDRESS (*City, State, and ZIP Code*)
8a NAME OF FUNDING / SPONSORING ORGANIZATION Space and Naval Warfare Systems Command 8b OFFICE SYMBOL (*If applicable*) SPAWAR 05	9. PROCUREMENT INSTRUMENT IDENTIFICATION NUMBER
8c ADDRESS (*City, State, and ZIP Code*) Washington, D.C. 20363-5100	10 SOURCE OF FUNDING NUMBERS PROGRAM ELEMENT NO. 61152N; PROJECT NO R00001; TASK NO. RR0230101; WORK UNIT ACCESSION NO DN505142

11 TITLE (*Include Security Classification*)
Thermal Macrowake of Surface Ships

12 PERSONAL AUTHOR(S)
Cervenka, Peter O.

13a TYPE OF REPORT	13b TIME COVERED	14. DATE OF REPORT (*Year, Month, Day*)	15. PAGE COUNT
Final	FROM _____ TO _____	1988 February	36

16 SUPPLEMENTARY NOTATION

17 COSATI CODES		
FIELD	GROUP	SUB-GROUP

18. SUBJECT TERMS (*Continue on reverse if necessary and identify by block number*)
Wake · Remote sensing
Macrowake · Surface ships
Infrared wake

19 ABSTRACT (*Continue on reverse if necessary and identify by block number*)

A theoretical scheme to describe the infrared scar left by a surface ship on a body of water is presented. Starting from a field velocity distribution behind the vessel, the fluid mechanical behavior of the disturbance is developed as it interacts with the vertical thermal profile of the water and produces a temperature pattern on the sea surface. As a result, the signal sensed by a remote detection system is obtained.

A detailed sensitivity study of the computational results is conducted by separately varying each of the main code variables. This method yields program input values that best fit the measurements.

Using a bell-shaped velocity distribution as an input, the contrast radiant intensity of a natural macrowake generated by a catamaran is computed to be -225 kW/sr. This compares with a measured value of -298 kW/sr, from which it differs by about 24%.

The variation of the spatial width of the macrowake on the water surface is computed, and found to fit the measurements. An infrared gap is sometimes observed at the onset of the macrowake. Actual imagery of a catamaran and a monohull ship shows definite evidence of gaps. Gap extents can be predicted by the theory to better than 5% accuracy. Keywords:

20 DISTRIBUTION / AVAILABILITY OF ABSTRACT	21 ABSTRACT SECURITY CLASSIFICATION
☒ UNCLASSIFIED/UNLIMITED ☐ SAME AS RPT ☐ DTIC USERS	Unclassified
22a NAME OF RESPONSIBLE INDIVIDUAL Peter O. Cervenka	22b TELEPHONE (*Include Area Code*) (202) 227-1591 22c. OFFICE SYMBOL Code 1412

DD FORM 1473, 84 MAR 83 APR edition may be used until exhausted
All other editions are obsolete

SECURITY CLASSIFICATION OF THIS PAGE
UNCLASSIFIED

A

CONTENTS

FIGURES

FIGURES (Continued)

TABLES

ABSTRACT

A theoretical scheme to describe the infrared contrast field left by a surface ship on a body of water is presented. Starting from a field velocity distribution behind the vessel, the fluid mechanical behavior of the disturbance is developed as it interacts with the vertical thermal profile of the water and produces a temperature pattern on the sea surface. As a result, the signal sensed by a remote detection system is obtained.

A detailed sensitivity study of the computational results is conducted by separately varying each of the main code variables. This method yields program input values that best fit the measurements.

Using a bell-shaped velocity distribution as an input, the contrast radiant intensity of a natural macrowake generated by a catamaran is computed to be −225 kW/sr. This compares with a measured value of −298 kW/sr, from which it differs by about 24%.

The variation of the spatial width of the macrowake on the water surface is computed, and found to fit the measurements. An infrared gap is sometimes observed at the onset of the macrowake. Actual imagery of a catamaran and a monohull ship shows definite evidence of gaps. Gap extents can be predicted by the theory to better than 5% accuracy.

ADMINISTRATIVE INFORMATION

This project was supported by the David Taylor Research Center (DTRC) Independent Research Program, sponsored by the Space and Naval Warfare Systems Command, Director of Navy Laboratories, SPAWAR 005, and administered by the Research Coordinator, DTRC 012.3 under Program Element 61152N, Task Area ZR-000-01-01 and DTRC Work Unit 2960-011.

INTRODUCTION

Whenever a surface ship moves across a body of water, it leaves behind it a characteristic pattern that can be observed for many kilometers. Detection is achieved through the application of a number of techniques, including: visible photography, acoustics, conventional radar, synthetic aperture radar, microwave radiometry and infrared sensing, which is the subject of the present report.

Four distinct regions characterize the macrowake. Just behind the ship, it begins as foamy, aerated and turbulent water. The bow wave originated by ship motion, the turbulent boundary layer adjacent to the hull, and the effect of the propeller all produce large amounts of foam.

Following the initial spreading is a region known as the turbulent core. In this region, no significant production of white water occurs, although many bubbles are still to be found at and below the surface. If the upper layer of the sea is thermally stratified, then the violent mixing that takes place in the turbulent core will bring to the surface some water which is at a different temperature. The temperature difference between the fluid inside the contrast field and the surrounding water makes the macrowake detectable by an infrared radiometer. After the disappearance of the foam, the turbulent core remains visually distinct from the surrounding ocean surface because of its slick appearance. This second region ends when there is no longer a visual distinction between the ocean surface and the macrowake.

Small bubbles still remain in the thermally-mixed water of the third region, and the temperature remains different from that of the surrounding water.

In the final stage, bubbles in the turbulent core have disappeared, but the thermally mixed water at the surface has not returned to the state of thermal equilibrium that existed before the passage of the ship. When it does, the contrast field can no longer be detected.

Some pioneering work in wake analysis can be traced back to the Second World War.[1] Unfortunately, most measurements performed since then lack instrument calibration as well as any sea-truth information. On the theoretical side, a thorough search of the literature has failed to uncover any previous attempt at a mathematical understanding of the infrared signal generated by the macrowake of surface ships.

The surface manifestation of the macrowake starts out as a three-dimensional flow pattern within the water. This situation is conceptually depicted in Fig. 1. When real measurements are simulated with a computer, the flow can be made to interact with a vertically stratified ocean. The in-band contrast radiant intensity of the macrowake is then calculated at various distances. The close range value is compared with the measured data. The spatial width of the macrowake is compared to the corresponding image data. In addition to presenting the details of an actual simulation, this paper concludes with a calculation of the thermal gap that is sometimes observed behind surface ships.

METHOD

The main features of interest are the temperature profile, the spatial width of the macrowake on the free surface, and the contrast signal generated by the infrared macrowake at a remote sensor system. All these quantities can be readily compared with accurate measurements.

The principal measurements used in the present work were gathered during the Phelps Bank microwave experiment, which was conducted to investigate the anomalous observations made by the SEASAT satellite.[2,3] Mr. P. M. Smith of the Naval Ocean Research and Development Activity, kindly provided a number of digitized infrared images of the oceanographic research ship *Hayes* and its macrowake. Mr. Smith also sent us an image of the macrowake generated behind the surveying ship *Kane*, taken a few years earlier in the Sargasso Sea.[4]

The details of the analysis can be followed in the block diagram of Fig. 2. In this analysis, velocity data from a vertical plane behind the propeller and vertical water density information are read by the computer. A fluid mechanical code propagates the flow in three dimensions within the water. This method eventually generates a temperature map of the water. The pattern on the free surface can be translated by the detector module into a contrast signal. The inclusion of the atmospheric propagation yields the infrared signal as it is received by a remote sensor.

A subsurface wake program called GORWAK[5] was used for the fluid mechanical code. This code solves the inviscid two-dimensional equations for the evolution of a density and flow disturbance in a stratified ocean environment. It uses a finite-difference numerical integration of the Euler equations in the vorticity-stream-function representation. The GORWAK description includes the surface and bottom of the ocean.

Despite obvious advantages, the use of this program also involves possible problems. One may question the suitability of using a subsurface code in modeling a surface contrast

field as is the case in the infrared. Another concern is that an underwater wake is essentially momentumless, while a surface ship generates an "ordinary" wake, which is one where mixing and air entrainment occur.

SIMULATION

Consider a situation in which the sea is described in terms of a number of layers. Displacing a vertical column of the fluid infinitesimally from its position of equilibrium gives rise to a natural frequency of oscillation. This frequency is called the Brunt-Vaisala frequency[6] and is defined by the expression

$$N^2 = -\left(\frac{g}{\varrho_0}\right)\left(\frac{\partial \bar{\varrho}}{\partial z}\right) \tag{1}$$

where

- N = Brunt-Vaisala frequency in rad/s
- g = gravitational acceleration in cm/s^{-2}
- z = vertical distance expressed in cm
- ϱ_0 = reference density at the free surface $z = 0$ and
- $\bar{\varrho}$ = mean density at z.

Near the surface, one may consider that

$$\partial \bar{\varrho} \approx \partial \varrho_0 \cdot \tag{2}$$

Equation 1 can now be rewritten as

$$N^2 = -\left(\frac{g}{\varrho_0}\right)\left(\frac{\partial \varrho_0}{\partial T}\right)\left(\frac{\partial T}{\partial z}\right) \tag{3}$$

where T is the temperature in °C. Since the thermal expansivity α is given by

$$\alpha = \frac{1}{\varrho_0}\left(\frac{\partial \varrho_0}{\partial T}\right) \cdot \tag{4}$$

Equation 3 becomes

$$N^2 = -g\,\alpha\left(\frac{\partial T}{\partial z}\right) \cdot \tag{5}$$

Density values for ordinary water at temperatures between 10 and 20°C may be obtained from standard sources.[7] The thermal expansivity α thus obtained is equal to $0.00015°C^{-1}$. This value corresponds to a Brunt-Vaisala frequency equal to 0.0012 rad/s.

In the GORWAK right-handed coordinate system, positive x is the direction parallel to the sea surface away from the stern. Positive y is starboard of a person standing on the deck and facing the bow of the ship. As indicated above, the positive z axis points to the local zenith. In order to simulate the measurements of Garrett and Smith[2], a temperature decrease of 1°C for every 10 m of increased water depth is assumed throughout the simulation. As the depth increases, the increments of both T and z are negative. Their ratio is positive and may be expressed as

$$\left(\frac{\partial T}{\partial z}\right) = 0.1°C/m \tag{6}$$

RESULTS

Making use of a bell-shaped velocity profile, the code was test-run for several depths of the wake axis below the free surface. The axis of the wake was taken from a depth of 20 m to about 10 m below the surface. Preliminary results showed that, for wake axis depths shallower than 10 m, water warmer than the warmest found in the whole profile appeared right at the surface, clearly a meaningless result.

It was then realized that GORWAK performs a smoothing (porosity) interpolation both at the water surface and at the ocean floor, possibly causing some anomalous results at these boundaries. These suspicions were fully confirmed. By-pass of the interpolation immediately corrected the problem, yielding physically meaningful results for wake depths as shallow as 2 m. With this first difficulty successfully overcome, a series of runs was made to confirm the code could accurately describe the behavior of the macrowake.

A word about nomenclature: we noticed that the data we received were labelled differently from those of Garrett and Smith.[2] In an effort to maintain consistency with the published literature, we inquired as to the discrepancy and were informed by Smith in a private communication that each of the two authors has adopted his own system of wake identification. The one used in their paper is due to W. D. Garrett. The identification of the wakes adopted in the present paper is the one used by P. M. Smith and found on the data tapes we received from him.

Program input data are listed in two tables. Table 1 contains the density profile, in oceanographic sigma units, as a function of water depth. Table 2 contains most of the other important parameters used in the same simulation. The results of the simulation are extracted from computer file BL375.R6.

The data in Figs. 3 through 13 correspond to a time span of 13.50 minutes. They represent the time evolution within a vertical plane which is perpendicular to the axis of the wake. Swirl is given a value of zero. The problem is symmetrical and only the right half of the plane is shown. A number of additional results, such as the vorticity and stream functions, are listed in the output but are not shown here.

The GORWAK output is expressed in terms of density increments which must be translated into temperature changes. The density of sea-water is generally a function of temperature, pressure, and salinity. The persistence of the macrowake is of the order of a few hours. The time constant associated with temperature changes at sea is of the order of hours. On the other hand, salinity does not change appreciably for days. Hence, for the practical purpose of this study, the salinity is assumed to be a constant equal to 35 parts per thousand. This number is a realistic average value of ocean salinity.[8] Equation 4 can then be written as follows

$$\delta\varrho = (\alpha \times \varrho)\, \delta T. \tag{7}$$

When the values of the expansivity and the density near the surface are known, each incremental density change corresponds to one value of the temperature difference. Thus, a temperature difference of 1 °C corresponds to a density change of 0.000172 or 1.72×10^{-4}. Figures 3 through 13 are drawn to represent temperature differences. Note that an infrared scanner sees only the vicinity of the top horizontal line in the plots, which represents the free surface.

Table 1. Density profile for macrowake run BL375.R6.

Depth (m)	0	100	190	200
Density	24.72	26.44	27.00	27.10

Note: Density values are in oceanographic units of sigma.

Table 2. Main input parameters of macrowake run BL375.R6.

Variable Name	Description	Value
ACCUR	Accuracy parameter	0.5
BOTTOM	Bottom depth	10000 m
IDEPB = IDEPT	Wake depth	3.7 m
IPROFL	Vertical density profile	(measured = 3)
PARMIX	Mixing parameter	0.8
PORZ	Smoothing at surface and bottom	0
SWIRL	Amount of swirl	0
TOTTIM	Converts to time through formula	5
WKRDFF	Wake radius	10 m

Following the P. M. Smith wake identification scheme already mentioned, we investigate the thermal characteristics of Wake 7. We divide the contrast field into nine flat rectangular elements. The length of each rectangle is equal to the distance between the profiles.[9] The width of the rectangular pieces is equal to the width of the corresponding profiles. The temperature of each rectangular element is the average of the corresponding profile.

We now make use of another computer program called SIRS.[10] This code is designed to generate the thermal characteristics of ships. Vessels under study are divided into a number of flat pieces. In order to model the wake, we substitute the rectangular elements described above for the flat elements of a ship. It must be stressed that the only parts of SIRS that are used in this application are the atmospheric propagation and the detector modules. The temperature of the flat pieces is computed by GORWAK rather than SIRS. Using parts of SIRS as we did was dictated purely by convenience. Other techniques could have been used and might have performed equally well. The measured and theoretical wake results are compared in Table 3.

Table 3. The signal from Wake 7.

MEASUREMENT				THEORY	
Vert. nmi	Range km	Contrast Radiant Intensity W/sr	Contrast Irradiance W/cm^2	Contrast Radiant Intensity W/sr	Contrast Irradiance W/cm^2
1	2	−0.298E+06	−0.867E−05	−0.225E+06	−0.655E−05
5	9	−0.273E+06	−0.318E−06	−0.206E+06	−0.240E−06
10	19	−0.270E+06	−0.786E−07	−0.204E+06	−0.594E−07
20	37	−0.267E+06	−0.194E−07	−0.202E+06	−0.147E−07
50	93	−0.267E+06	−0.311E−08	−0.202E+06	−0.235E−08
100	185	−0.267E+06	−0.778E−09	−0.202E+06	−0.588E−09
200	371	−0.267E+06	−0.194E−09	−0.202E+06	−0.147E−09
300	556	−0.267E+06	−0.864E−10	−0.202E+06	−0.653E−10

SENSITIVITY ANALYSIS

A sensitivity analysis of the GORWAK computer code shows how strongly each of the principal factors affects the results and which particular characteristics of the macrowake are affected. Table 4 lists, starting from the left-hand column, the physical quantities, their corresponding variable name, the program default value, the value used in the calculation, and the name of the file that contains the computation results. Referring back to Table 2, it may be remembered that file BL375.R6 contains the results of the closest fit simulation.

The variables that are being examined are: the macrowake linear velocity (VWAKE), the radial steepness (ANURAD), the radius (WKRDFF), and the distance between the propeller axis and the free water surface (IDEPB = IDEPT). For each parameter, the macrowake profile is shown at three distances from the stern: 516 m, 1485 m, and 2295 m, respectively. The VWAKE results are contained in Figs. 14, 15, and 16. The ANURAD variations are plotted in Figs. 17, 18, and 19. The effect of varying the macrowake radius WKRDFF is shown in Figs. 20, 21, and 22. Finally, the influence of the propeller depth is displayed in Figs. 23, 24, and 25. In Figs. 14 through 25, line plots indicate measured data. They are shown superimposed on best fit results.

Another program variable describes swirl (and goes by the name SWIRL). A number of simulation runs have been performed to examine its effects, which in general are quite important, on the macrowake. However, a study of the measured data does not show any unsymmetrical features that may be attributed to swirl. For this reason, as Table 2 shows, the SWIRL variable has been set equal to zero for the present simulation.

Table 4. Sensitivity analysis outline.

Factor	Name	Default	Value this Run	File Name
Wake Linear Velocity	VWAKE	0 cm/s	0 cm/s	DM05.R6
		0 cm/s	2 cm/s	BL375.R6
		0 cm/s	10 cm/s	BL374.R6
Wake Radial Steepness	ANURAD	4	2	BL375.R6
		4	4	DM04.R6
		4	6	DM03.R6
Wake Radius	WKRDFF	10 m	5 m	BL377.R6
		10 m	10 m	BL375.R6
		10 m	15 m	BL381.R6
		10 m	20 m	DM08.R6
Propeller Depth	IDEPB = IDEPT	—	2 m	BLP2.R6
		—	3.7 m	BL375.R6
		—	10 m	DM10.R6
		—	20 m	DM12.R6

SENSITIVITY TO THE LINEAR SPEED OF THE MACROWAKE (VWAKE)

The shape of the macrowake is highly sensitive to the linear speed. Figures 15 (c) and 16 (c) show that a speed of 10 cm/s causes two thermal spikes to appear at a temperature that is higher than any other found in the thermal profile. This nonphysical situation is a limiting case. A careful variation of VWAKE reveals that a speed of 2 cm/s results in the best fit with the measured data.

SENSITIVITY TO THE SHAPE OF THE VELOCITY FIELD (ANURAD AND WKRDFF)

The ANURAD variable describes how sharply the velocity falls off in the radial direction, while WKRDFF is an effective macrowake radius, measured in meters. These two variables describe the shape of the velocity field. Figures 19 and 22 show that in the far field, the macrowake profile is sensitive to changes in the shape of the velocity distribution.

Starting from an examination of the macrowake, one may ponder whether it is possible to draw any inferences regarding the characteristics of the ship that is producing it. In its present shape, the GORWAK code starts from a field velocity distribution input. In order to find an answer to the important practical problem just posed, some effort will be required if we are to correlate our macrowake results with the design parameters of the ship.

SENSITIVITY TO THE PROPELLER DEPTH (IDEPB)

The effect on the macrowake of changing the propeller depth can be seen in Figs. 23 through 25, as IDEPB is varied from 2 m to 20 m beneath the free water surface. The shape of the macrowake profile is quite sensitive to this variable. During the simulation, IDEPB is set to a value of 3.7 m, which is the design depth of the *Hayes* propellers below the sea surface.

Figure 23 depicts a macrowake profile caused by a propeller at a depth of 20 m. A small scar is detectable at a distance of 516 m behind the stern. No contrast field appears either at 1485 m (see Fig. 24) or at 2295 m (see Fig. 25).

DISCUSSION

MODEL ACCURACY

The overall deviation between calculated and measured values in Table 3 is about 24%. Two factors conspire to make the agreement somewhat worse than it ought to be.

First, the vertical thermal profile for Wake 7 was measured at least two days before the infrared imagery was gathered. Smith says* that the change in the profile over these 48 hours cannot be estimated.

Second, the GORWAK program explicitly expects the local thermal background to be essentially static during the measurement. The underlying assumption is that two spatial dimensions plus the time coordinate are equivalent to three spatial dimensions. The time variable is related to the distance behind the ship via a constant linear speed, equal to 4.71 m/s for the *Hayes*. Several clues indicate that the infrared background of the data used is active. The thermal profiles of Fig. 26 are distorted to the right, starting some 2295 m behind the stern, possibly due to a front pushing the macrowake to the right. The photograph representing the full extent of the measured macrowake clearly shows the presence of a sharp thermal front at the end of the wake.[11]

This disturbance notwithstanding, the agreement between measurement and theory is still acceptable. Hence, it seems that the program can be relied upon to yield accurate results even in the presence of a certain level of disturbance, as long as the macrowake is not distorted in some catastrophic manner.

THE MACROWAKE SHAPE AND SPATIAL WIDTH

Figure 26 compares computational data with measured ones. Plots (a) through (f) have only one minimum. Plot (g) reveals the sudden appearance of a double dip. The computed macrowake, shown on the same graph, goes through a similar double minimum at exactly the same moment.

The computer-generated spatial width of the macrowake, drawn in Fig. 27 as a continuous line, is compared with measured data represented by black dots. Good agreement is obtained everywhere except for the last point. This anomaly may be explained by the sudden appearance of the thermal front already mentioned.

---

* P. M. Smith, in a private communication.

GORWAK simulation results have also been compared with macrowake width calculations contained in a study of the interaction between microwave radar and the turbulent wake.[12] Some of the computations contained in that report are applicable to the wake of a small (Class 1) ship of 5000 tons. The *Hayes* is in the same weight category, since its full load displacement is equal to 3860 tons.[13] Swanson's results are in agreement with the values displayed in Fig. 27.

THE MACROWAKE GAP

Next is a test of the near-field behavior of the theory. Careful examination of the infrared imagery reveals that in some instances there is a gap at the onset of the macrowake, just behind the stern. Figure 28 is an enhanced photograph of the surveying ship with its wake. The gain settings on the infrared scanner made the signal from the macrowake just discernible: it was estimated* at about 0.5°C. The length of the gap, measured on this photograph, is 275.5 m.

Figure 29 is a black-and-white photograph of a false-color coded image of the *Hayes* and Wake 8. The dark temperature contour closest to the stern corresponds to a temperature difference of 0.1°C. The next contour, light in color, represents a temperature difference of 0.5°C. For comparison with the previous photograph, the contour at 0.5°C is considered. The distance between the stern and the 0.5°C contour, measured on the photograph, is equal to 269.1 m.

The calculated maximum temperature contrast of the macrowake is plotted in Fig. 30 versus the distance (the contrast is negative). A contrast of 0.5°C corresponds to a distance of 283 m behind the ship. The measured gap length of the *Kane* deviates from the theory by 2.7%, the one on the *Hayes* differs by 4.9%.

CONCLUSIONS

Using a generic bell-shaped velocity distribution and no swirl, we have been able to simulate the infrared signal generated by the macrowake of a twin-hull surface ship, the *Hayes*, running only on its starboard engine. The contrast radiant intensity of the macrowake, the evolution and extent of the spatial width, and the gap length all fit the measurements. Impressive as the results are, we do not yet feel justified in making sweeping statements that apply to all surface ship wakes. At present, it must be remembered that only one macrowake measurement has been analyzed. The preceding results raise an interesting question. Figure 13 shows the presence of large finger-like components of the wake inside the water. Does such a flow pattern really occur in the wake? The only evidence we now have of that possibility appears in Reference 14. It is clear that careful detailed measurements are needed inside the water, down to depths of several tens of meters.

The experience gained in this project leads to the following criteria as a basis for making good quality infrared macrowake measurements. To be useful, infrared imagery should preferably

1. Be taken in a down-looking geometry, from an airborne platform flying along the axis of the wake and using a top quality calibrated stable infrared viewer.
2. Be accompanied by a vertical air and water temperature profile measured as closely as possible in time and space with the infrared data.

---

* P. M. Smith, in a private communication.

3. Include thermal profiles measured across the macrowake at several distances behind the ship and at equal depths up to about 50 m beneath the sea surface.

4. Include other data as well, such as information about the ship producing the wake, other accompanying wakes, ship hull design specifications, measurements of the flow field around the hull, propeller design, near-field propeller flow in front of and behind the propeller, ship engine power specifications, cooling and discharge temperatures, past thermal ship history and movements, oceanic currents, and possible presence of older wakes in the area.

Work on the other available infrared imagery has been started. It is unfortunate that we lack a measurement of the exact velocity distribution associated with the macrowakes mentioned in the present analysis. We also lack careful macrowake measurements on other ship types and classes, be they full-scale or to-scale models. We hope the present effort will encourage more research in this area and emphasize the need for careful gathering of some urgently needed measurements.

ACKNOWLEDGMENTS

The author wishes to express his appreciation to Mr. E. E. Rudd of the U. S. Naval Research Laboratory and to Dr. Glyn O. Roberts for providing him with a copy of the wake code.

Thanks are due to Mr. P. M. Smith, of the Naval Ocean Research and Development Activity, for making macrowake measurements available and to Mr. John Schmidt of the same laboratory who was responsible for the successful collection and digitization of the analog infrared imagery.

Dr. Warren C. Dietz, at the time Head of the DTRC Ship Systems Integration Department, and Mr. Dennis J. Clark, Assistant Technical Director for Development, kindly authorized the free use of a Digital Equipment Corporation VAX 11/730 computer. Their valuable contribution to this project is gratefully acknowledged.

Mr. Gerald G. Switzer, Department Head, Dr. Charles S. Weller, Head of the Observables Technology Division and Mr. Robert G. Stilwell, Head of Technology and Advance Programs, actively provided support for this research. The author also wishes to acknowledge useful discussions and expert help in the area of infrared simulation received from Mr. Robert H. Burns, Mr. Olin M. Pearcy and Mr. David L. Etherton.

Last but not least, none of this work could have been done without the deep interest, constant encouragement, and funding provided by Dr. David D. Moran, the DTRC Assistant Technical Director for Research.

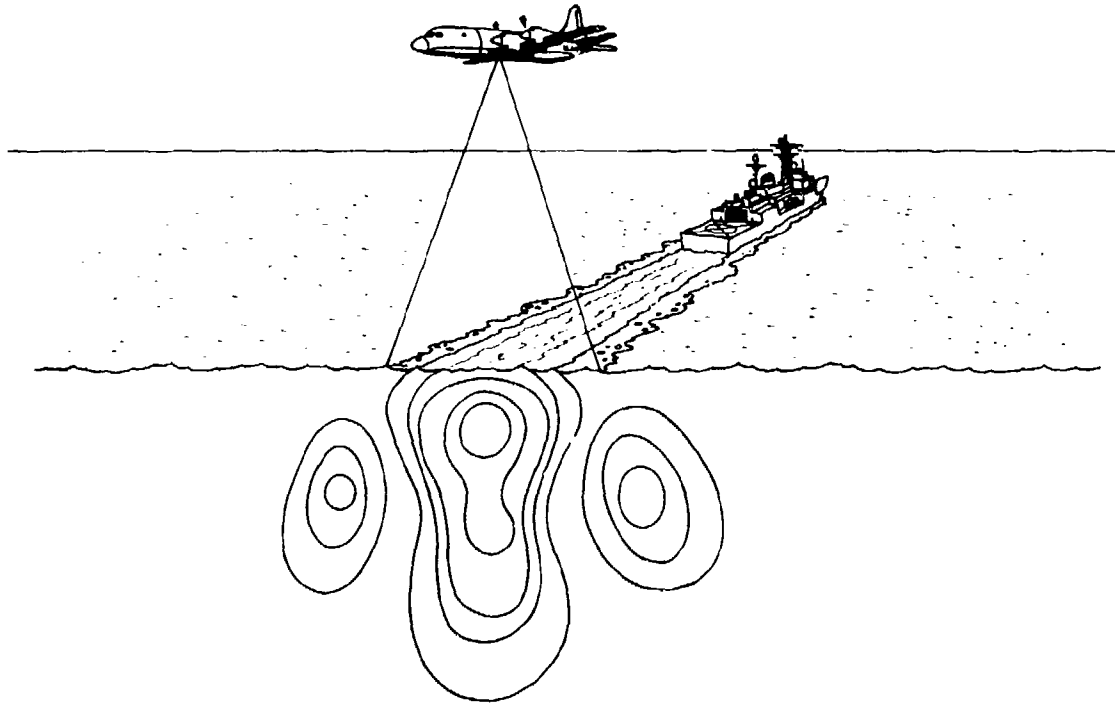

Fig. 1. The infrared surface ship macrowake problem. (The measurement instrumentation is flown on board the aircraft.)

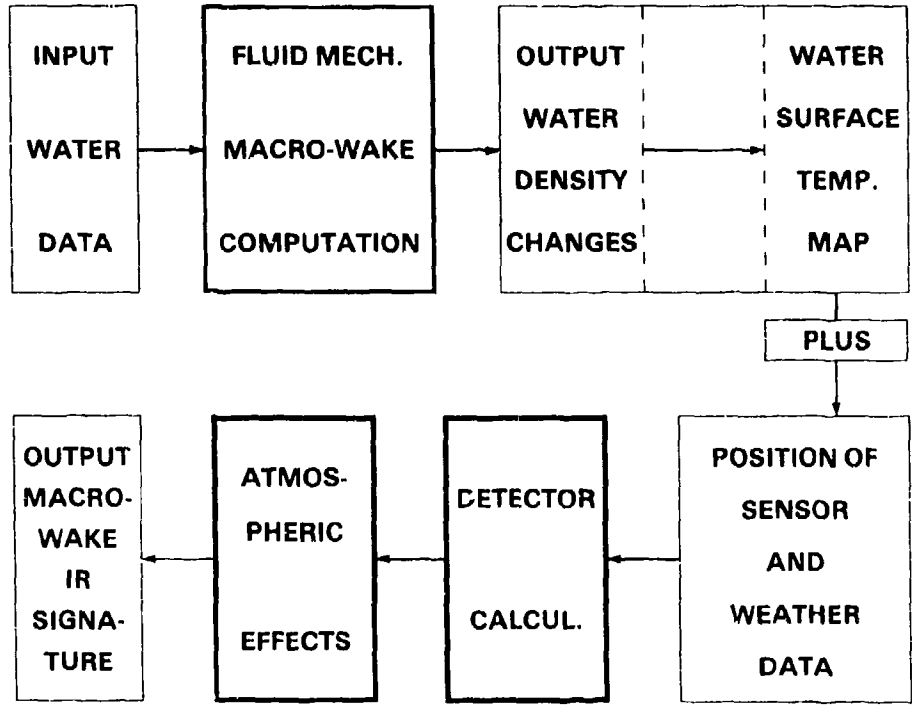

Fig. 2. Block diagram of the theoretical scheme.

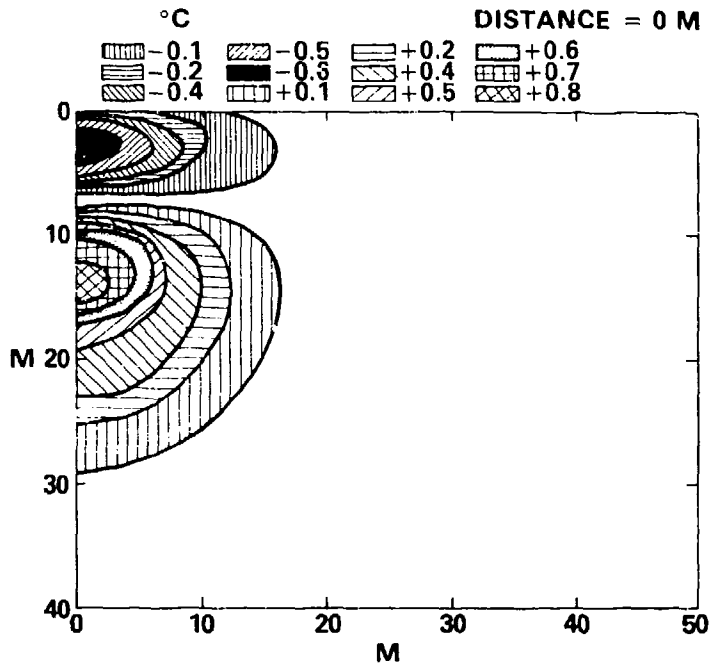

Fig. 3. The calculated temperature difference contours at 0.00 min. (Contours are displayed in a vertical section through the macrowake. The pattern is symmetrical about the left-hand side vertical axis.)

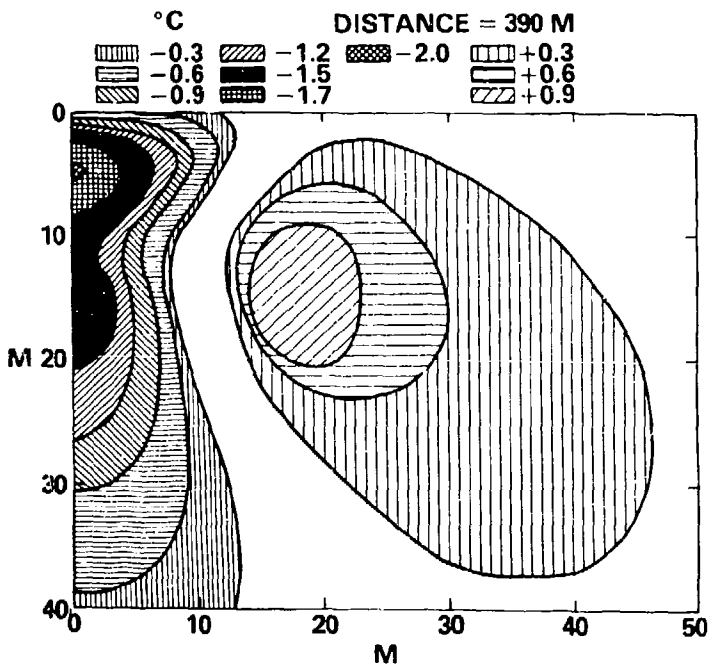

Fig. 4. The calculated temperature difference contours at 1.38 min. (Contours are displayed in a vertical section through the macrowake. The pattern is symmetrical about the left-hand side vertical axis.)

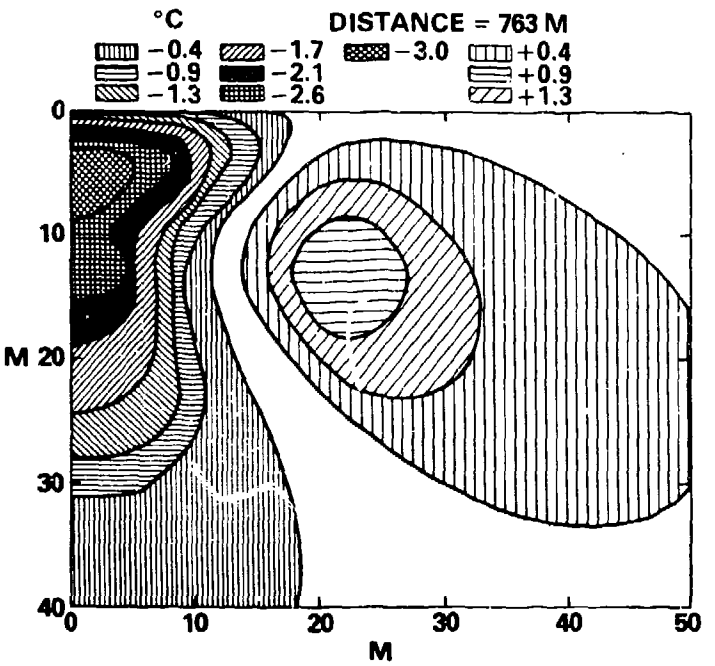

Fig. 5. The calculated temperature difference contours at 2.70 min. (Contours are displayed in a vertical section through the macrowake. The pattern is symmetrical about the left-hand side vertical axis.)

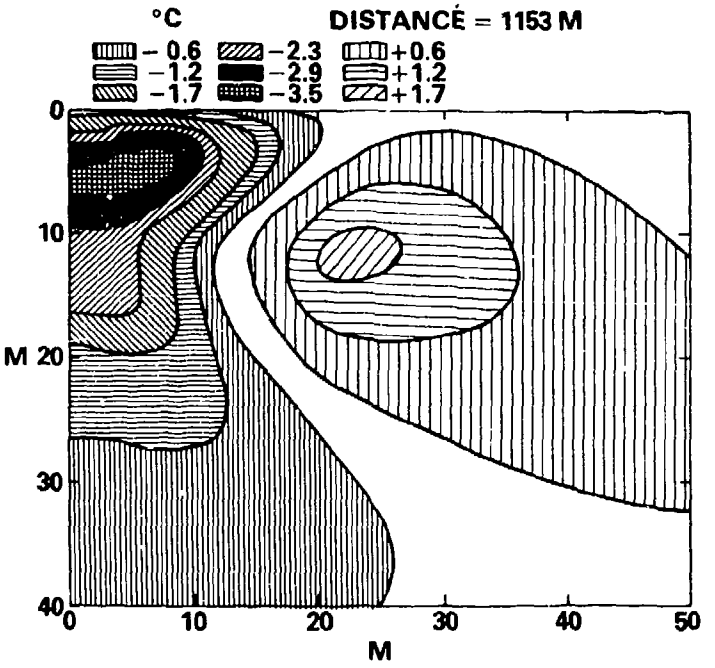

Fig. 6. The calculated temperature difference contours at 4.08 min. (Contours are displayed in a vertical section through the macrowake. The pattern is symmetrical about the left-hand side vertical axis.)

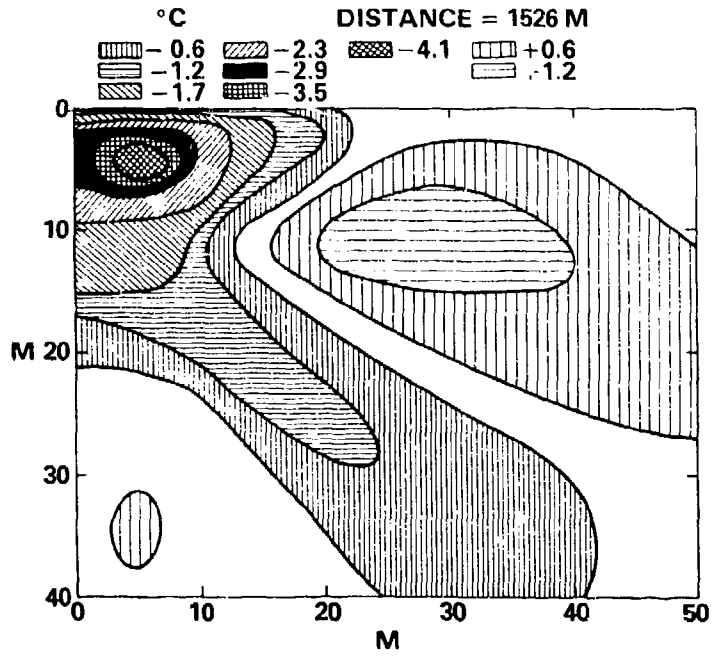

Fig. 7. The calculated temperature difference contours at 5.40 min. (Contours are displayed in a vertical section through the macrowake. The pattern is symmetrical about the left-hand side vertical axis.)

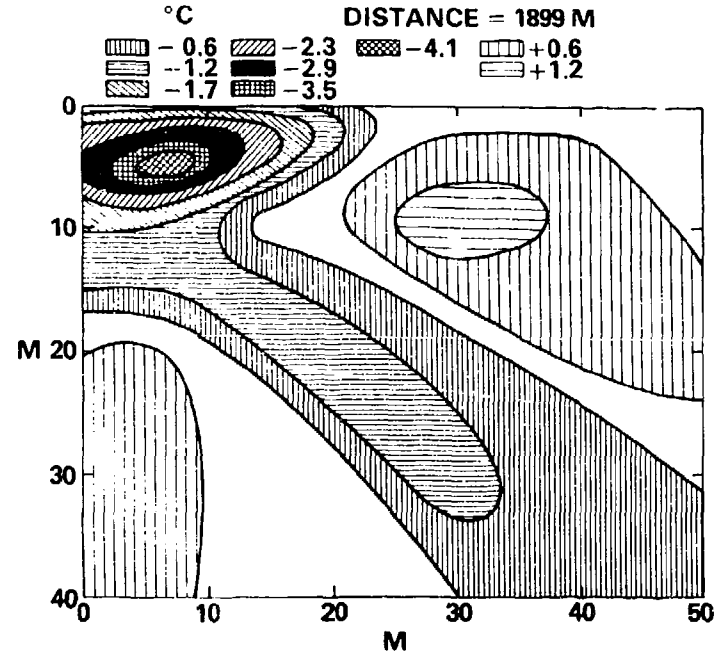

Fig. 8. The calculated temperature difference contours at 6.72 min. (Contours are displayed in a vertical section through the macrowake. The pattern is symmetrical about the left-hand side vertical axis.)

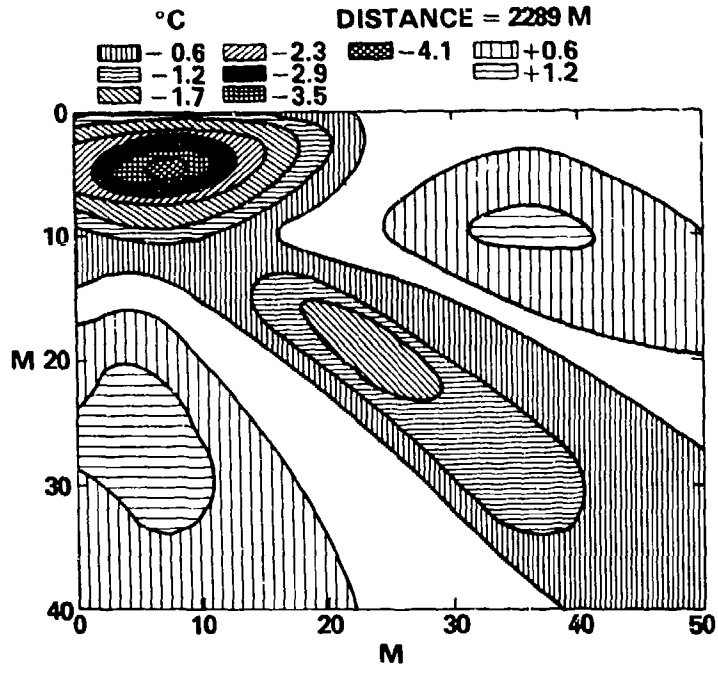

Fig. 9. The calculated temperature difference contours at 8.10 min. (Contours are displayed in a vertical section through the macrowake. The pattern is symmetrical about the left-hand side vertical axis.)

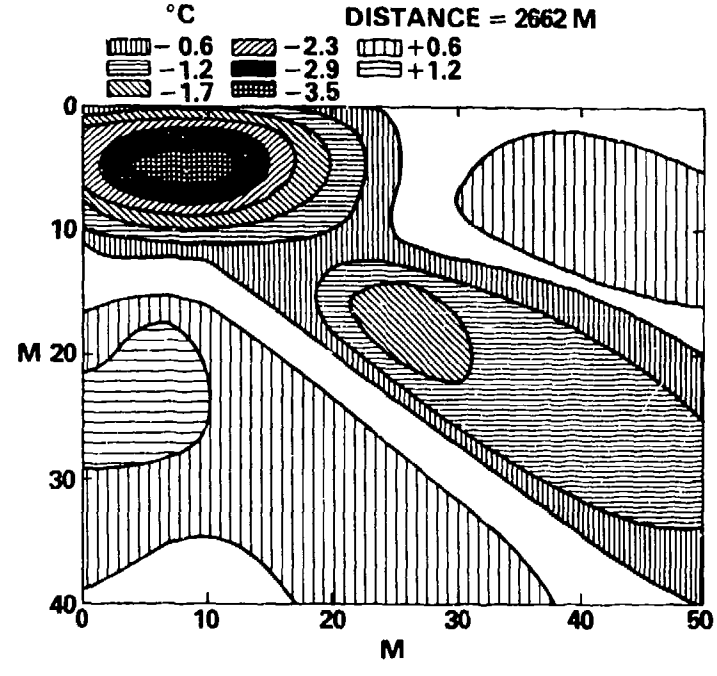

Fig. 10. The calculated temperature difference contours at 9.42 min. (Contours are displayed in a vertical section through the macrowake. The pattern is symmetrical about the left-hand side vertical axis.)

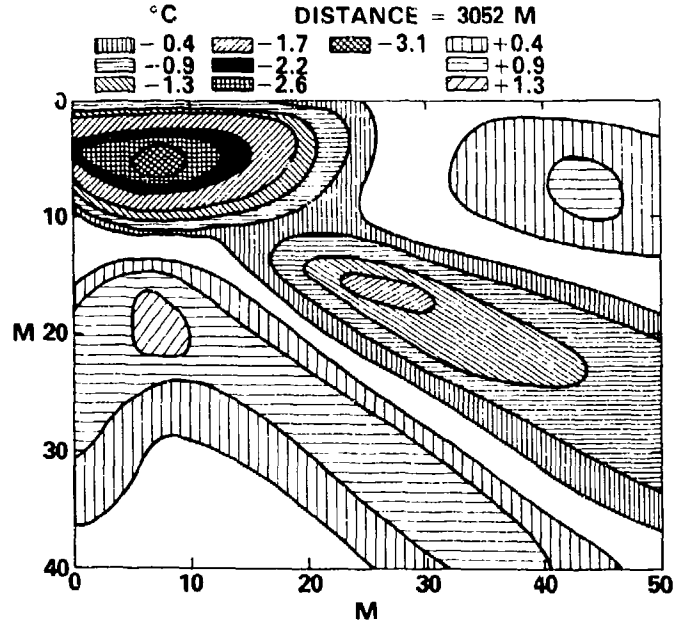

Fig. 11. The calculated temperature difference contours at 10.80 min. (Contours are displayed in a vertical section through the macrowake. The pattern is symmetrical about the left-hand side vertical axis.)

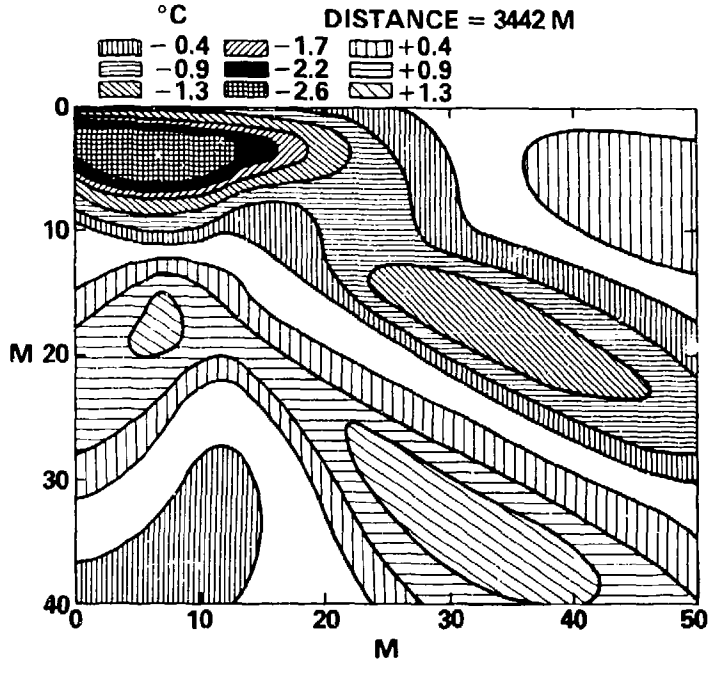

Fig. 12. The calculated temperature difference contours at 12.18 min. (Contours are displayed in a vertical section through the macrowake. The pattern is symmetrical about the left-hand side vertical axis.)

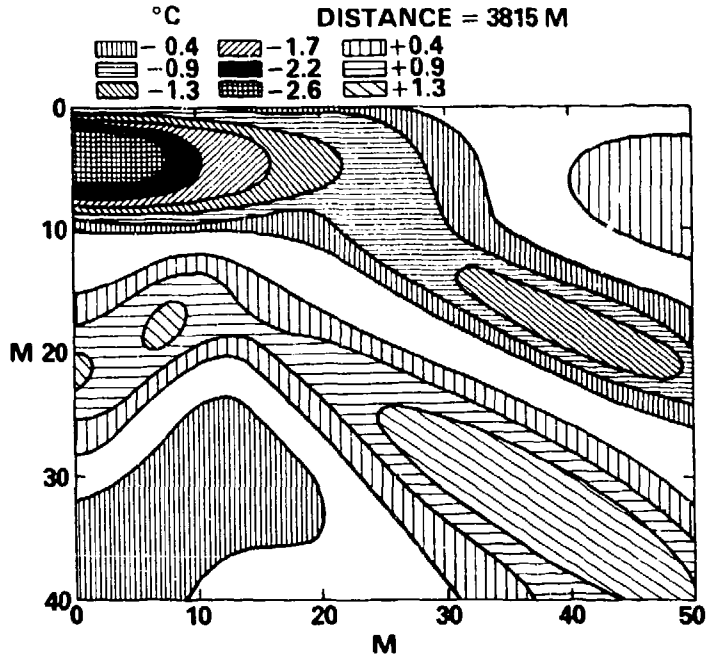

Fig. 13. The calculated temperature difference contours at 13.50 min. (Contours are displayed in a vertical section through the macrowake. The pattern is symmetrical about the left-hand side vertical axis.)

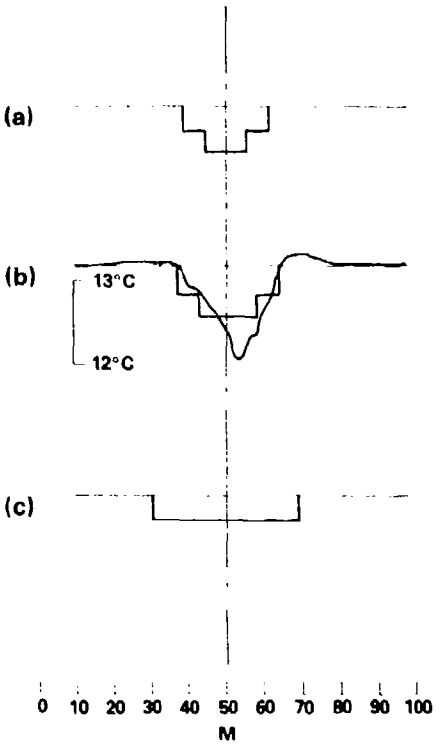

Fig. 14. The macrowake profile at 516 m with VWAKE equal to: (a) 0 cm/s, (b) 2 cm/s, (c) 10 cm/s.

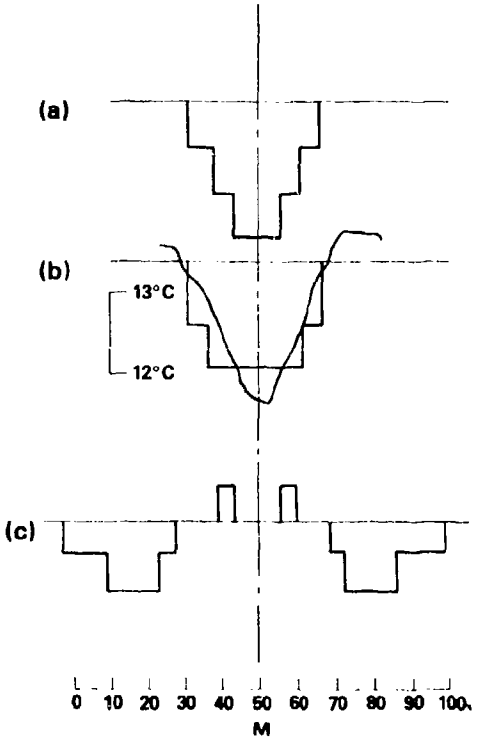

Fig. 15. The macrowake profile at 1485 m with VWAKE equal to: (a) 0 cm/s, (b) 2 cm/s, (c) 10 cm/s.

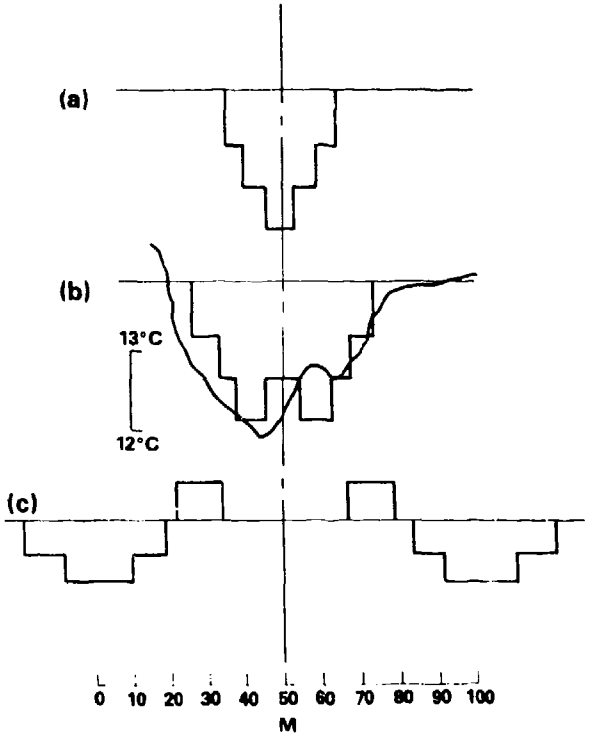

Fig. 16. The macrowake profile at 2295 m with VWAKE equal to: (a) 0 cm/s, (b) 2 cm/s, (c) 10 cm/s.

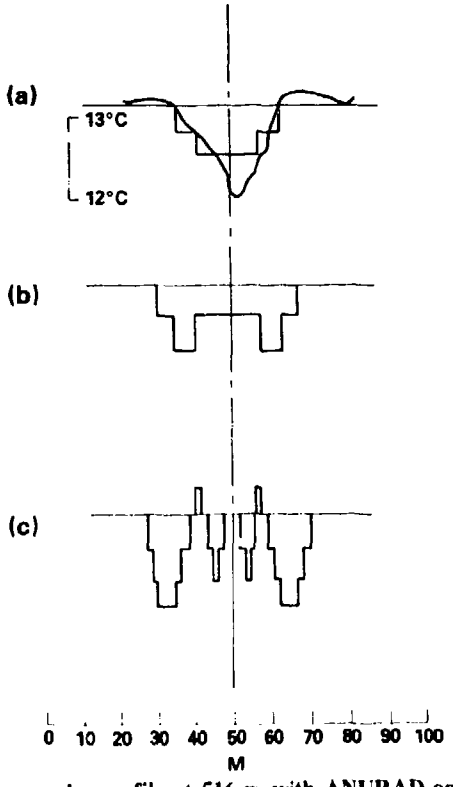

Fig. 17. The macrowake profile at 516 m with ANURAD equal to: (a) 2, (b) 4, (c) 10.

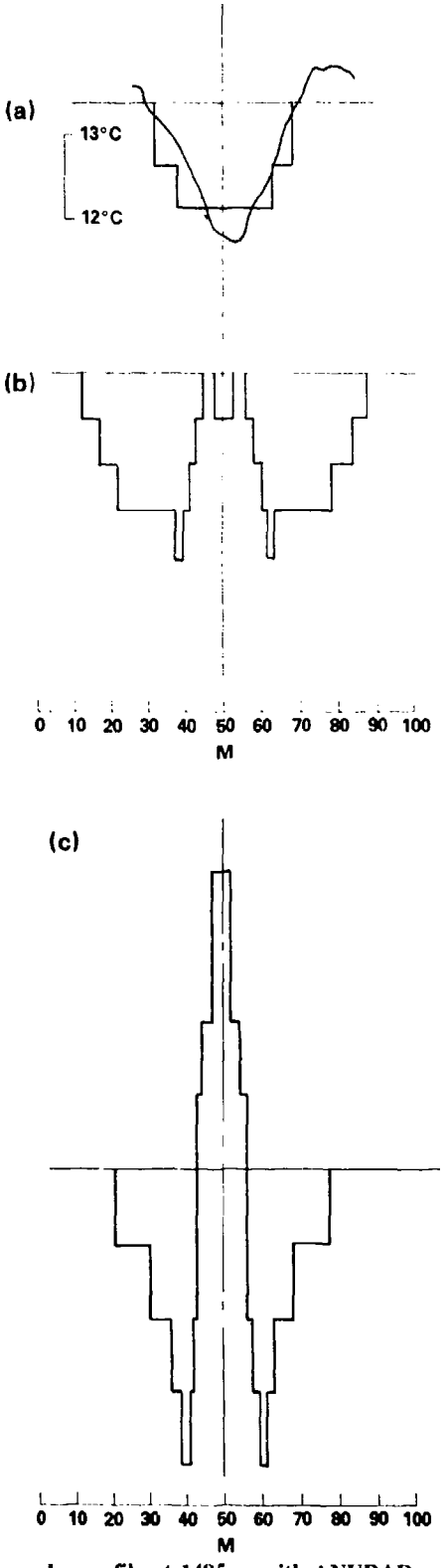

Fig. 18. The macrowake profile at 1485 m with ANURAD equal to: (a) 2, (b) 4, (c) 10.

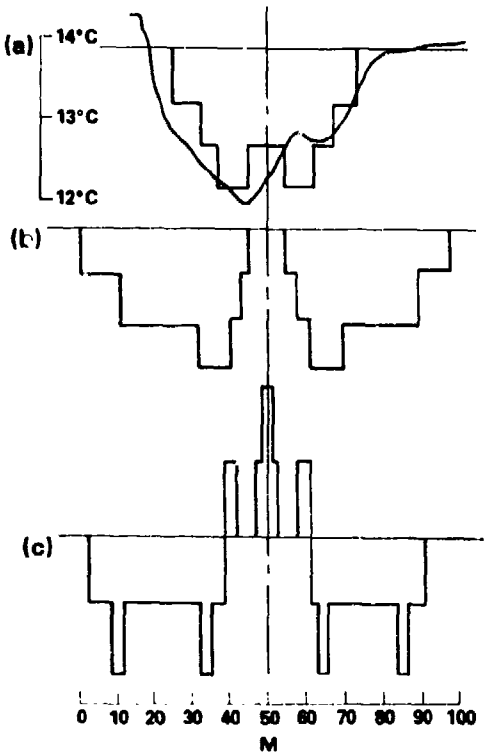

Fig. 19. The macrowake profile at 2295 m with ANURAD equal to: (a) 2, (b) 4, (c) 10.

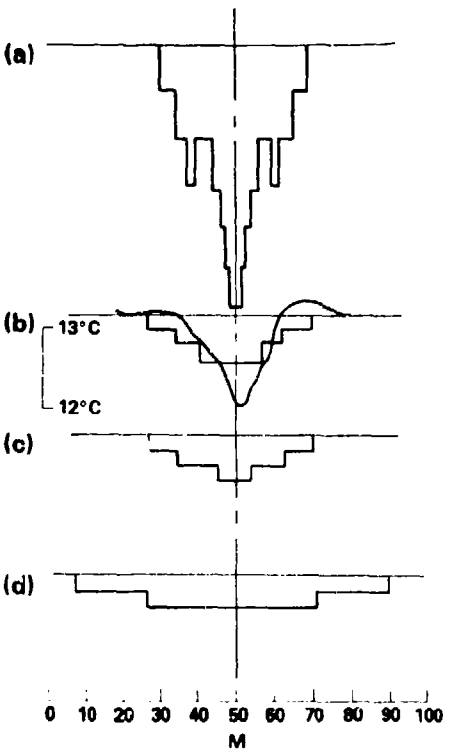

Fig. 20. The macrowake profile at 516 m with WKRDFF equal to: (a) 5 m, (b) 10 m, (c) 15 m, (d) 20 m.

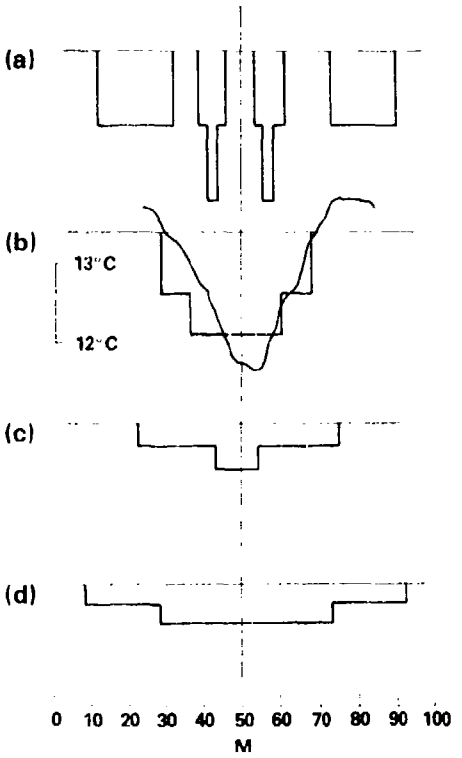

Fig. 21. The macrowake profile at 1485 m with WKRDFF equal to: (a) 5 m, (b) 10 m, (c) 15 m, (d) 20 m.

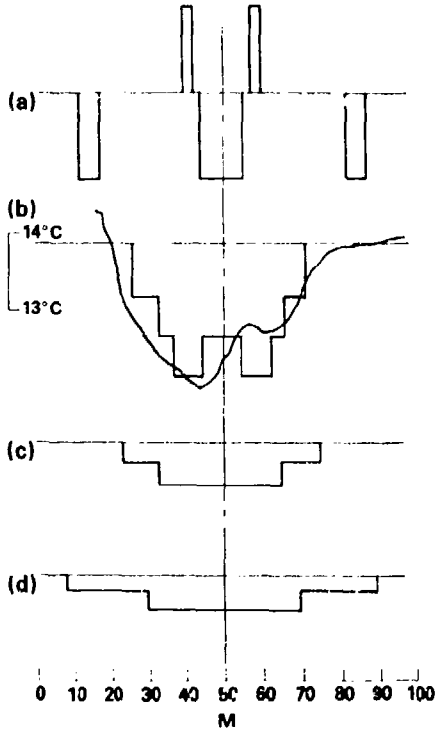

Fig. 22. The macrowake profile at 2295 m with WKRDFF equal to: (a) 5 m, (b) 10 m, (c) 15 m, (d) 20 m.

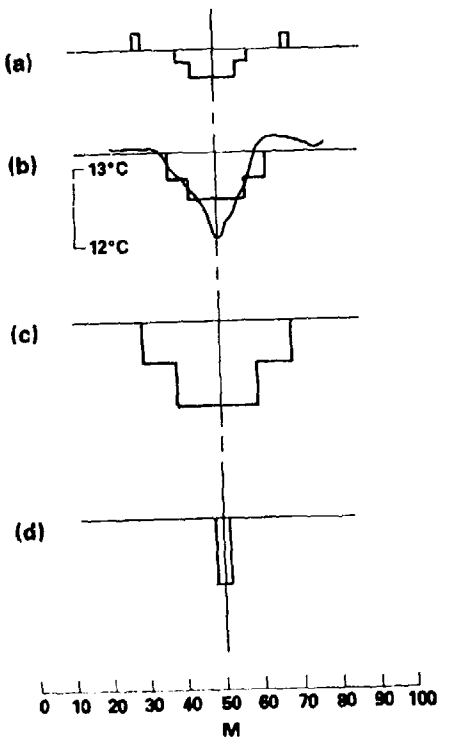

Fig. 23. The macrowake profile at 516 m and propeller depth of: (a) 2 m, (b) 3.7 m, (c) 10 m, (d) 20 m.

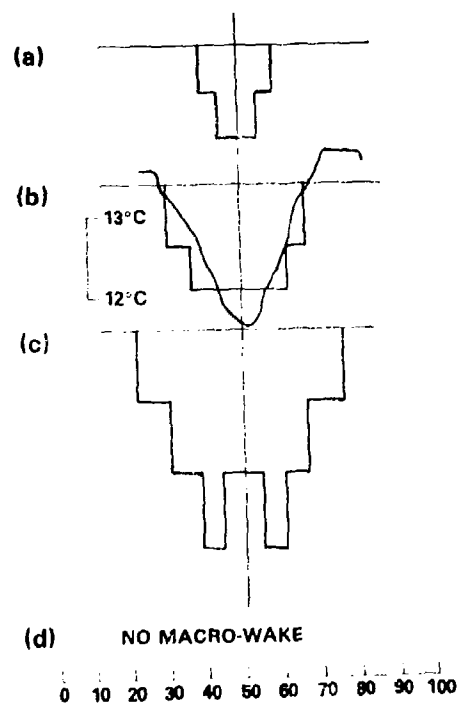

Fig. 24. The macrowake profile at 1485 m and propeller depth of: (a) 2 m, (b) 3.7 m, (c) 10 m, (d) 20 m (no macrowake appears).

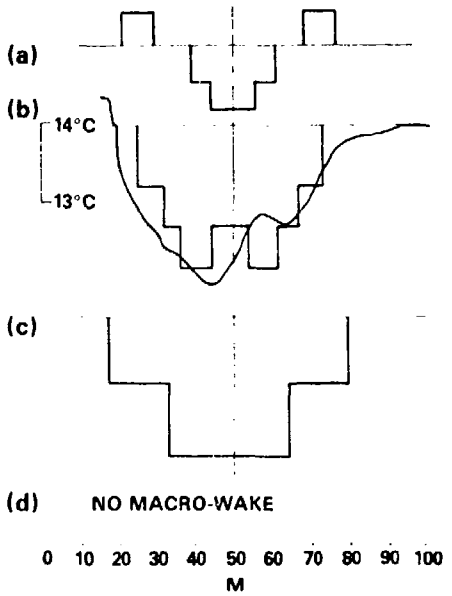

Fig. 25. The macrowake profile at 2295 m and propeller depth of: (a) 2 m, (b) 3.7 m, (c) 10 m, (d) 20 m (no macrowake appears).

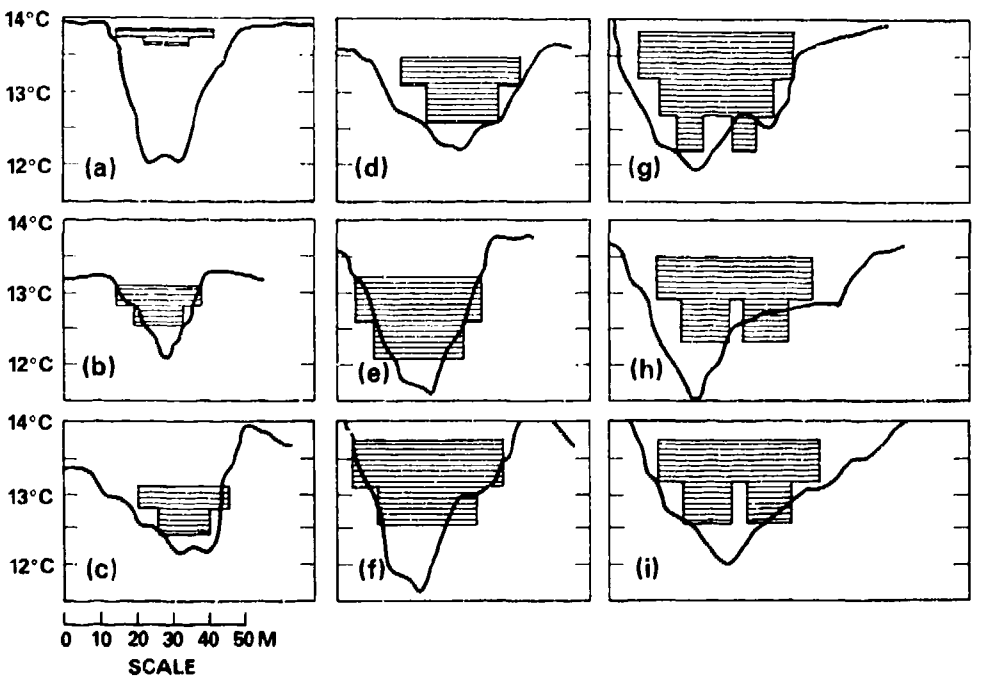

Fig. 26. Comparison of the Wake 7 measured profiles (drawn with a continuous line) with theoretical calculations (drawn with a hash mark). The corresponding times or distances from the stern of the *Hayes* are: (a) 1.1 min. or 311 m (b) 1.83 min. or 516 m (c) 2.47 min. or 697 m (d) 3.93 min. or 1110 m (e) 5.25 min. or 1485 m (f) 6.69 min. or 1890 m (g) 8.12 min. or 2295 m (h) 9.54 min. or 2695 m (i) 10.86 min. or 3070 m.

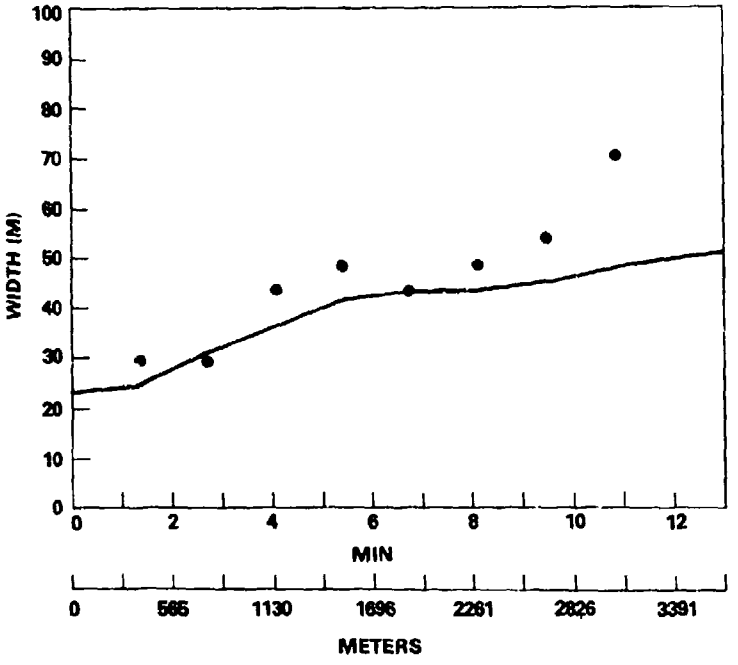

Fig. 27. The spatial width measured across Wake 7 on the free surface (drawn with a continuous line), compared with the calculated values (shown as full dots). The macrowake was generated by the *Hayes*.

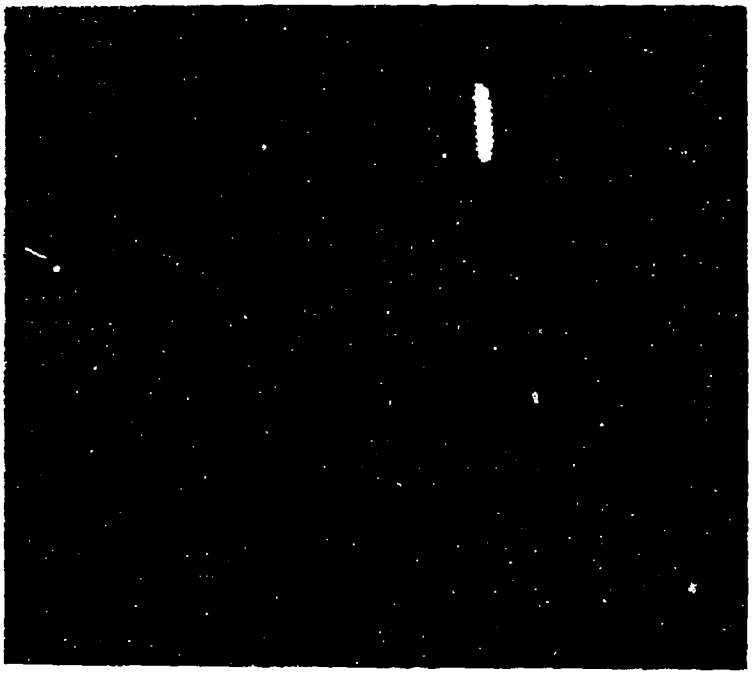

Fig. 28. A digitally enhanced photograph shows the *Kane* and part of the macrowake it generates. (Notice the gap in this 8 to 12 micrometer band image.)

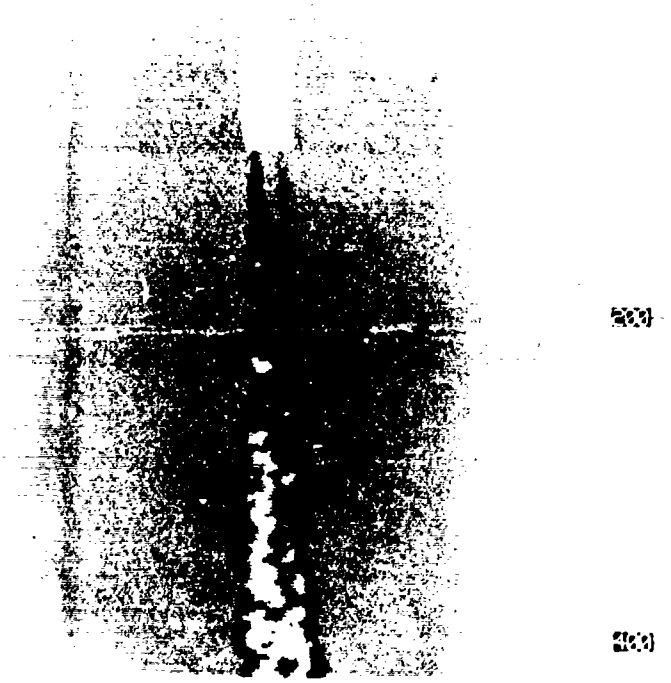

Fig. 29. Black-and-white reproduction of a digitally-enhanced false color image of the *Hayes*, showing the beginning of Wake 8. (Note the gap behind the starboard engine. The port engine is turned off.)

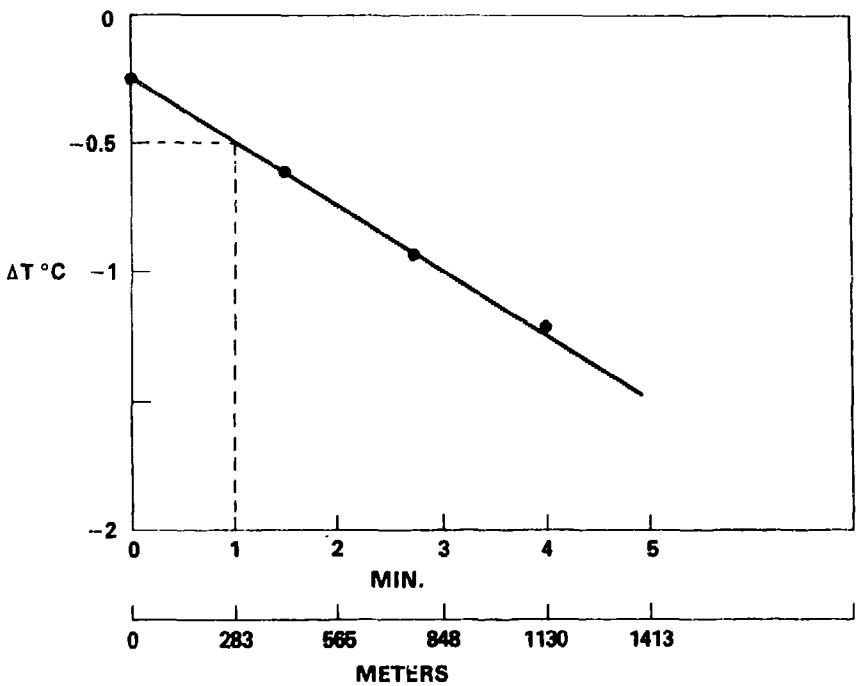

Fig. 30. Plot of the calculated near-field temperature contrast of the macrowake, as a function of the distance from the stern. (Numerical values are taken from file BL375.R6.)

REFERENCES

1. Garber, D. H., R. J. Urick, and J. Cryden, "Thermal Wake Detection," Defense Technical Information Center Document AD 493 809, Navy Electronics Lab., San Diego, CA (Jan 1945).

2. Garrett, W. D., and P. M. Smith, "Physical and Chemical Factors Affecting the Thermal IR Imagery of Ship Wakes," Naval Research Laboratory Memorandum Report 5376 (26 Jul 1984).

3. Peltzer, R. D., "Remote Sensing of the U. S. N. S. Hayes Wake," Naval Research Laboratory Memorandum Report 5430 (28 Sep 1984).

4. "Oceanic Environmental Background Observations in the Sargasso Sea During September 1979," H. Perkins, Ed., Naval Ocean Research and Development Activity Technical Note 58 (Mar 1980).

5. Roberts, G. O., and D. M. Rubenstein, "Shear Effects on Internal Gravity Wave Propagation," Science Applications, Inc. Report SAI-80-973-WA (12 Jun 1980).

6. Phillips, O. M., "*The Dynamics of the Upper Ocean*," second edition, p. 18, Cambridge University Press, Cambridge, U.K. (1980).

7. "*Handbook of Chemistry and Physics*," Weast, R. C., ed., 55th edition, p. F-5, CRC Press, Cleveland, OH (1974-75).

8. Sverdrup, H. U., M. W. Johnson, and R. H. Fleming, "*The Oceans*," p. 55, Prentice-Hall, NY (1942).

9. Garrett, W. D., and P. M. Smith, "Physical and Chemical Factors Affecting the Thermal IR Imagery of Ship Wakes," p. 12, Fig. 6 (the natural wake), Naval Research Laboratory Memorandum Report 5376 (26 Jul 1984).

10. Battey, P. E., "Ship Infrared Computer Model Technical Overview and User's Manual," DTNSRDC Report 79/093 (Sep 1979).

11. Garrett, W. D., and P. M. Smith, "Physical and Chemical Factors Affecting the Thermal IR Imagery of Ship Wakes," p. 7, Fig. 2 (the untreated wake), Naval Research Laboratory Memorandum Report 5376 (26 Jul 1984).

12. Swanson, C. V., "Radar Observability of Ship Wakes," p. 21, Fig. 9, Cortana Corporation Report (11 May 1984).

13. "*Jane's Fighting Ships*," Capt. J. Moore, Ed., p. 775, Jane's Publishing Co. Ltd., London, U.K. (1986-87).

14. Garber, D. H., R. J. Urick, and J. Cryden, "Thermal Wake Detection," Defense Technical Information Center Document AD 493 809, Plate 4, Navy Electronics Lab., San Diego, CA (Jan 1945).

INITIAL DISTRIBUTION

Copies

1 OUSDR&E/J.M. MacCallum

2 CNO
- 1 Code 35E, L. Triggs
- 1 Code 276, CAPT R. Barr

2 NAVAIR
- 1 Code 5164L, P.W. Wyman
- 1 Lib

7 NAVSEA
- 1 SEA 05, RADM Ricketts
- 1 SEA 05MB, LCDR Stone
- 1 SEA 05R22, A. Johnson
- 1 SEA 55X12, T. Ulinski
- 1 SEA 61XB, CAPT S. Pryzby
- 1 SEA 0039, A. Ritter
- 1 Lib

1 SPAWAR/Code PDW107, L. Moskowitz

2 ONR
- 1 M. Blizard
- 1 R.D. Whiting

3 NADC
- 1 Code 3011, S.B. Campana
- 1 Code 3011, M.R. Hess
- 1 Code 3011, H.L. Sokoloff

3 NORDA
- 1 Code 321, A.S. Green
- 1 Code 321, P.M. Smith
- 1 Code 321, J. Schmidt

1 NOSC/Code 743, J. Fitchek

8 NRL
- 1 Code 4310, E.E. Rudd
- 1 Code 5800, R. Swim
- 1 Code 5300, A. Petty
- 1 Code 6500, T.G. Giallorenzi
- 1 Code 6520, J.C. Kershenstein
- 1 Code 6520, R. Priest
- 1 Code 6520, I. Schwartz
- 1 Lib

1 NSWC/Code R-42, D. Wilson

Copies

1 AFGL/B. Sandford

12 DTIC

5 Library of Congress/Science and Tech. Div.

2 NASA
- 1 Scientific & Tech Info. Facility
- 1 R. Buchan

1 USNA/Tech Lib

1 Hunter College of the City University of New York/ Dept. of Chemistry, L. Massa

3 APL/Johns Hopkins U
- 1 R.A. Steinberg
- 1 D. Wenstrand
- 1 Lib

3 Institute for Defense Analysis
- 1 L. Bieberman
- 1 H. Wolfhard
- 1 M.J. Burns

1 Logicon/J.W. Rucker

1 MRJ, Inc./M. Watkins

2 ORI, Inc.
- 1 V. Scott
- 1 J. Whitting

3 Photon Research Assoc., Inc.
- 1 C.A. Acquista
- 1 D. Anding
- 1 C. Ludwig

3 W.J. Schaeffer & Assoc.
- 1 D. Friedman
- 1 J. Stregak
- 1 P.B. Ulrich

CENTER DISTRIBUTION

Copies	Code	Name
1	00	C. Graham
1	01	R. Metrey
1	01A	D.D. Moran
1	01B	D.J. Clark
1	011	E. O'Neill
5	0113	W. Lukens
1	0117	B. Nakonechny
1	12	G. Kerr
1	1222	G.W. Peters
1	14	G.G. Switzer
1	1401	R.G. Stilwell
1	1402	R.G. Allen
1	1410	C.S. Weller
1	1411	R.H. Burns
1	1411	M. Goldberg
1	1411	O.M. Pearcy
1	1411	C.R. Schumacher
25	1412	P.O. Cervenka
1	1412	M.A. Sekellick
1	15	W.B. Morgan
1	1506	S. Hawkins
1	1522	M.B. Wilson
1	1522	T.J. Nagle
1	154	J.H. McCarthy
1	1542	T.T. Huang
1	1542	L.P. Purtell
1	1543	E.P. Rood
1	1543	D.W. Coder
1	1544	A.M. Reed
1	1620	R.J. Furey
1	1802	H.J. Lugt
1	1840	J.W. Schot
1	1843	H. Haussling
1	2833	M. Greenberg
10	5211.1	Reports Control
1	522.1	TIC (C)
1	522.2	TIC (A)